Electronic excitation of dielectronic targets by ion impact

Gustavo H. Olivera, César A. Ramírez,* and Roberto D. Rivarola*

*Instituto de Física de Rosario, Consejo Nacional de Investigaciones Científicas y Técnicas
and Universidad Nacional de Rosario, Avenida Pellegrini 250, 2000 Rosario, Argentina*

A symmetric eikonal model is developed to study the electron excitation of dielectronic atomic targets by impact of bare nuclei. An independent-electron approximation is used, where one of the electrons, the *passive* one, is assumed to remain frozen during the reaction. The influence of the passive electron on the trajectory followed by the projectile is determined in calculating the differential cross sections. Total cross sections are also computed and compared with available experimental data for the impact of different projectiles with He, Fe^{24+}, and Kr^{34+} targets.

PACS number(s): 34.50.Fa

I. INTRODUCTION

In the present work we focus our study on the single-electron excitation of dielectronic atomic targets by impact of bare heavy ions at intermediate ($v \sim v_e$) and high ($v \gg ve$) energies. Here v and v_e are the collision velocity and the initial orbital velocity of the excited electron, respectively. With such a goal in mind we use a symmetric eikonal (SE) approximation as employed previously for monoelectronic targets [1,2]. It is considered that one of the electrons, the active one, is excited while the other one remains passive as if frozen during the collision. The influence of the passive electron on the active one is included in the entry and exit channels through the use of variational calculations that determine the initial and final bound wave functions representing the active electron. The interaction between the projectile and the passive electron and the internuclear potential are taken into account by means of the introduction of static potentials. These static potentials, which appear in the exponential phases multiplying the bound wave functions on both channels, influence the trajectory of the projectile. The use of static potentials has been previously introduced to study single-electron capture [3], single-electron ionization by impact of bare ions on multielectronic targets [4], and single-electron excitation by impact of one-electron projectiles on monoelectronic targets [5]. In this last case the frozen passive electron is traveling with the projectile, and even though it does not affect the representation of the initial and final stationary wave function of the active electron, it contributes to the perturbative potential that provokes the excitation. In the present case the excitation is caused only by the perturbation produced by the projectile, and the passive electron affects solely the initial and final active electron distributions.

portance for the *linear energy transfer* (LET) occurring in the irradiation of biological matter by fast beams of bare heavy nuclei [6]. Our future interest is oriented on the determination of the influence of target excitation in the LET process.

The role of the interaction between the projectile and the passive electron is analyzed by comparing theoretical calculations with experimental differential cross sections for impact of protons on He targets. Total cross sections are also determined for this system.

Furthermore, total cross sections for impact of different neutral projectiles on the dielectronic multicharged Fe^{24+} and Kr^{34+} ions are computed and compared with existing experimental data. This will allow us to estimate the adequacy of the present independent-electron symmetric eikonal approximation to represent reactions where heavy multicharged targets are involved.

Atomics units will be used throughout except where otherwise indicated.

II. THEORY

We use the straight-line version of the impact-parameter approximation to study the single-electron excitation of a dielectronic atomic target of nuclear charge Z_T by impact of a bare nucleus of charge Z_P. Let us indicate with $x_a (x_p)$ and $s_a (s_p)$ the position of the active (passive) electron, referred to a reference frame fixed on the target nucleus and projectile, respectively. The internuclear vector R gives the position of the projectile with respect to the target nucleus. In these coordinates, the time-dependent Schrödinger equation, which describes the evolution of the collision system, results in

$$\left[H - i\frac{\partial}{\partial t} \right] \Psi_{i,f}^{\pm}(x_a, x_p, t)$$
$$= \left[\sum_{k=a}^{p} \left[-\frac{1}{2}\nabla_{x_k}^2 - \frac{Z_T}{x_k} - \frac{Z_P}{s_k} \right] + \frac{1}{|x_a - x_p|} \right.$$
$$\left. + \frac{Z_P Z_T}{R} - i\frac{\partial}{\partial t} \right] \Psi_{i,f}^{\pm}(x_a, x_p, t) = 0 . \tag{1}$$

In Eq. (1), H represents that total Hamiltonian and Ψ_i^{+} (Ψ_f^{-}) is the associated *exact* initial (final) wave function verifying outgoing (incoming) asymptotic conditions. For simplicity of formulation we describe the reaction

from an inertial frame fixed on the target nucleus (the recoil of the target is neglected and the approximation $M_{P,T} \gg 1$ is used, with M_P and M_T being the nuclear masses of the projectile and of the target, respectively). Let us assume that the passive electron remains frozen during the collision, so that we can write

$$\Psi_i^+(\mathbf{x}_a, \mathbf{x}_p, t) = \psi_i^+(\mathbf{x}_a, t)\varphi_p(\mathbf{x}_p) , \quad (2)$$

$$\Psi_f^-(\mathbf{x}_a, \mathbf{x}_p, t) = \psi_f^-(\mathbf{x}_a, t)\varphi_p(\mathbf{x}_p) , \quad (3)$$

where $\varphi_p(\mathbf{x}_p)$ is the (time-independent) bound-state wave function describing the passive electron in the initial or final state. The complete time dependence of the exact wave function $\Psi_{i,f}^\pm$ is contained in ψ_i^+ and ψ_f^-, which verify the Schrödinger equation

$$\left[\tilde{H} - i\frac{\partial}{\partial t} \right] \psi_{i,f}^\pm(\mathbf{x}_a, t) = 0 , \quad (4)$$

where $\tilde{H}$ is the Hamiltonian obtained as the average of the total Hamiltonian over the passive electron wave function φ_p

$$\tilde{H} = \langle \varphi_p | H | \varphi_p \rangle$$

$$= -\tfrac{1}{2}\nabla_{\mathbf{x}_a}^2 - \frac{Z_T}{x_a} - \frac{Z_P}{s_a} + V_{ap}(\mathbf{x}_a) + V_s(\mathbf{R}) + \epsilon_p . \quad (5)$$

In Eq. (5), $V_{ap}(\mathbf{x}_a)$ is then the effective potential acting upon the active electron due to its interaction with the passive one. It is given by

$$V_{ap}(\mathbf{x}_a) = \left\langle \varphi_p \left| \frac{1}{|\mathbf{x}_a - \mathbf{x}_p|} \right| \varphi_p \right\rangle . \quad (6)$$

$V_s(\mathbf{R})$ is the static potential including the interaction of the projectile with the passive electron and with the target nucleus, so that

$$V_s(\mathbf{R}) = \frac{Z_P Z_T}{R} - \left\langle \varphi_p \left| \frac{Z_P}{s_p} \right| \varphi_p \right\rangle . \quad (7)$$

Also, in Eq. (5), ϵ_p represents the part of the atomic energy corresponding only to the passive electron

$$\epsilon_p = \left\langle \varphi_p \left| -\tfrac{1}{2}\nabla_{\mathbf{x}_p}^2 - \frac{Z_P}{x_p} \right| \varphi_p \right\rangle . \quad (8)$$

Using the phase transformations

$$\psi_i^+(\mathbf{x}_a, t) = \Phi_{a,i}^+(\mathbf{x}_a, t)\exp(-i\epsilon_p t)$$

$$\times \exp\left\{ -i\int_{-\infty}^t V_s(\mathbf{R}')dt' \right\} , \quad (9)$$

$$\psi_f^-(\mathbf{x}_a, t) = \Phi_{a,f}^-(\mathbf{x}_a, t)\exp(-i\epsilon_p t)$$

$$\times \exp\left\{ i\int_t^{+\infty} V_s(\mathbf{R}')dt' \right\} , \quad (10)$$

the Schrödinger equation is reduced to the simple form

$$\left[H_a - i\frac{\partial}{\partial t} \right]\Phi_{a,j}^\pm(\mathbf{x}_a, t)$$

$$= \left[-\tfrac{1}{2}\nabla_{\mathbf{x}_a}^2 - \frac{Z_T}{x_a} + V_{ap}(\mathbf{x}_a) - \frac{Z_P}{s_a} - i\frac{\partial}{\partial t} \right]\Phi_{a,j}^\pm(\mathbf{x}_a, t)$$

$$= 0 \quad (11)$$

with $j = i, f$.

The wave function $\Phi_{a,i}^+$($\Phi_{a,f}^-$) will evolve with the initial (final) orbital energy of the active electron, with the asymptotic limits [7]

$$\lim_{t\to-\infty} \Phi_{a,i}^+ \longrightarrow \varphi_a^i(\mathbf{x}_a)\exp\left\{ -i\frac{Z_P}{v}\ln(vR - v^2t) \right\}$$

$$\times \exp(-i\epsilon_i t) , \quad (12)$$

$$\lim_{t\to+\infty} \Phi_{a,f}^- \longrightarrow \varphi_a^f(\mathbf{s}_a)\exp\left\{ +i\frac{Z_P}{v}\ln(vR + v^2t) \right\}$$

$$\times \exp(-i\epsilon_f t) , \quad (13)$$

and where $\varphi_a^i(\mathbf{x}_a)$ [$\varphi_a^f(\mathbf{s}_a)$] is the initial [final] active electron-orbital wave function and $\epsilon_i[\epsilon_f]$ is the corresponding initial [final] active electron-orbital energy.

If we choose the distorted initial and final wave functions as prescribed by the symmetrical eikonal approximation for monoelectronic targets [1], we obtain

$$\chi_i^+ = \varphi_a^i(\mathbf{x}_a)\exp\left\{ -i\frac{Z_P}{v}\ln(vs_a + \mathbf{v}\cdot\mathbf{s}_a) \right\}\exp(-i\epsilon_i t) \quad (14)$$

and

$$\chi_f^- = \varphi_a^f(\mathbf{s}_a)\exp\left\{ +i\frac{Z^P}{v}\ln(vs_a - \mathbf{v}\cdot\mathbf{s}_a) \right\}\exp(-i\epsilon_f t) , \quad (15)$$

which explicitly verify the asymptotic limits (12) and (13), respectively.

The impact-parameter-dependent first-order amplitude results [4,8] in

$$\mathcal{A}_{if}^-(\boldsymbol{\rho}) = \exp\left\{ -i\int_{-\infty}^{+\infty} V_s(\mathbf{R})dt \right\}a_{if}^-(\boldsymbol{\rho}) , \quad (16)$$

where

$$a_{if}^-(\boldsymbol{\rho}) = -i\int_{-\infty}^{+\infty} dt \left\langle \chi_f^- \left| H_a - i\frac{\partial}{\partial t} \right| \chi_i^+ \right\rangle \quad (17)$$

provided that

$$\lim_{t\to+\infty} \langle \Phi_{a,f}^- | \chi_i^+ \rangle = 0 . \quad (18)$$

The differential cross section is obtained by using the eikonal expression [9]

$$\frac{d\sigma}{d\Omega}=\mu^2v^2\left|\int_0^\infty d\rho\,\rho\mathcal{A}_{\mathrm{if}}^-(\rho)J_m\left[2\mu v\rho\sin\left(\frac{\theta}{2}\right)\right]\right|^2, \quad (19)$$

where J_m is the Bessel function of the first kind and of order m. m is the change in the magnetic quantum number between the initial and final states with the quantization axis taken along $\mathbf{v}$. Finally, μ is the reduced mass of the collision system and θ is the center-of-mass scattering angle.

Integrating over the impact parameter, the total cross section follows

$$\sigma=\int d\rho\,|\mathcal{A}_{\mathrm{if}}^-(\rho)|^2. \quad (20)$$

From Eqs. (19) and (20) it can easily be verified that the

exponential factor containing the static potential $V_s(\mathbf{R})$ influences $d\sigma/d\Omega$ but not σ.

III. CALCULATION OF THE SCATTERING AMPLITUDE

Let us consider that the stationary initial wave function representing the target in the fundamental state is described by a product of single-ζ hydrogenic functions.

The associated effective target nuclear charge Z_T^* is determined by using the variational method, so that $Z_T^*=Z_T-\frac{5}{16}$ and

$$\epsilon_i=\left\langle\varphi_a^i\left|H_a+\frac{Z_P}{s_a}\right|\varphi_a^i\right\rangle.$$

With this choice, the exponential factor appearing in expression (16) takes the form

$$\exp\left\{-i\int_{-\infty}^{+\infty}V_s(\mathbf{R})dt\right\}=\rho^{2i(Z_T-1)(Z_P/v)}\exp\left\{-\frac{2iZ_p}{v}[K_0(2Z_T^*\rho)+Z_T^*\rho K_1(2Z_T^*\rho)]\right\}\lim_{Z'\to\infty}\left[|2Z'|^{-2i(Z_T-1)(Z_P/v)}\right], \quad (21)$$

where K_0, K_1 are modified Bessel functions of the second kind. Except for constant phases [3,5], this exponential factor reduces at small and large impact parameter to

$$\lim_{\rho\to0}\exp\left\{-i\int_{-\infty}^{+\infty}V_s(\mathbf{R})dt\right\}\longrightarrow\rho^{(2iZ_TZ_P/v)}, \quad (22)$$

$$\lim_{\rho\to\infty}\exp\left\{-i\int_{-\infty}^{+\infty}V_s(\mathbf{R})dt\right\}\longrightarrow\rho^{2i(Z_T-1)Z_P/v}. \quad (23)$$

This means that for $\rho\to0$ and $\rho\to\infty$, the factors given by expressions (22) and (23) are simply the Rutherford amplitudes (in the eikonal approximation) describing the scattering between the bare nuclei ($\rho\to0$) and between the projectile and the target nucleus, screened by the passive electron ($\rho\to\infty$). In other words, (22) and (23) correspond to the potentials Z_TZ_P/R and $(Z_T-1)Z_P/R$ which are the limits of $V_s(R)$ as $R\to0$ and as $R\to\infty$, respectively.

The final orbital wave functions φ_a^f representing the active electron in different $n_f l_f m_f$ states are chosen to be hydrogenic functions, with variational charges and corresponding orbital energies, calculated by using the variational expression

$$\epsilon_f=\left\langle\varphi_a^f\left|H_a+\frac{Z_P}{s_a}\right|\varphi_a^f\right\rangle. \quad (24)$$

All these ingredients together allow then the scattering amplitude to be calculated from Eq. (16).

IV. RESULTS AND DISCUSSIONS

A. Impact of protons on helium atom

We study first the single-electron excitation of He targets by impact of protons at collision energies of 50 and

100 keV. The differential cross sections for the final state $nl=2p$ and the shell $n=2$ of the active electron calculated with the SE model are presented in Figs. 1 and 2. They are compared with the experimental data of Ref. [10]. The cross sections are evaluated with the scattering amplitude given by Eq. (16) and using three different exponential factors, namely Eq. (21) and its two asymptotic limits (22) and (23).

As only small scattering angles are considered, the differential cross section is dominated by large impact-parameter contributions. This fact is evident in Figs. 1
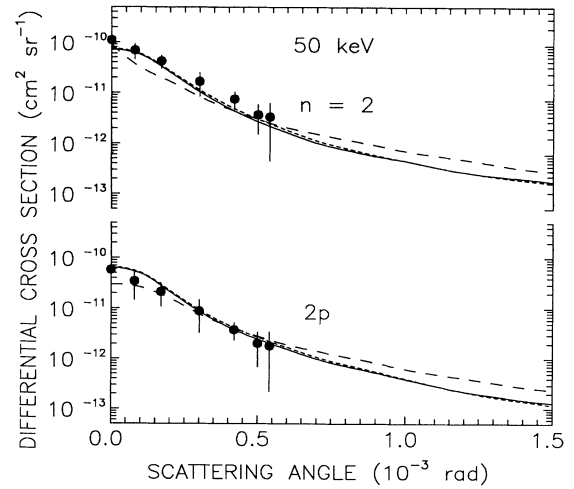

FIG. 1. Differential cross sections for the single excitation of He to state $nl=2p$ and to shell $n=2$ by the impact of H^+ at a 50-keV impact energy as a function of the scattering angle. Present theoretical results using different phase factors: solid line, Eq. (21); short-dashed line, Eq. (23); dashed line, Eq. (22). Experimental data: ●, from Ref. [10].
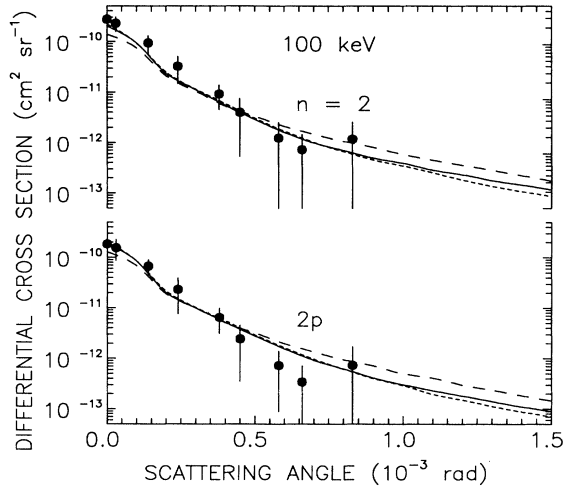
FIG. 2. Same as Fig. 1 but for 100-keV impact energy.

and 2, where the curves corresponding to the exponential factors of Eqs. (21) and (23) are very close. The comparison with the calculations obtained using Eq. (22), which is equivalent to describing the projectile trajectory only by the internuclear potential, shows us the influence of including the screening produced by the passive electron. The best agreement with experiments is obtained when the static potential $V_s(R)$ is used. We have repeated the calculations by using a five ζ-Roothaan Hartree-Fock wave function [11] to represent the initial bound state φ_a^i. The differences with respect to the single-ζ hydrogenic function are negligible. One also observes that the $n=2$ channel is dominated by the excitation of the active electron to the $2p$ level.

The importance of the inclusion of the exponential factor (associated with the static potential) in the scattering
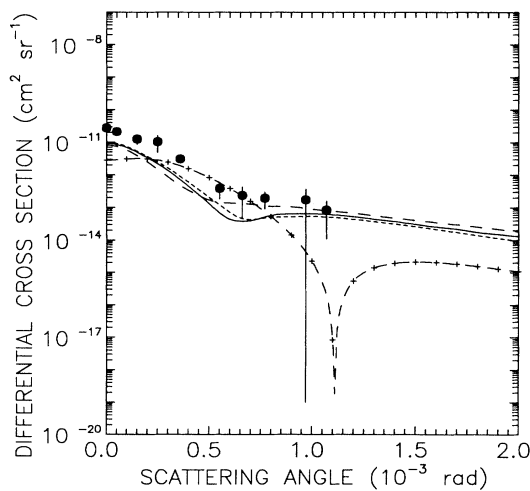

FIG. 3. Differential cross section for the single excitation of He to state $nl=2s$ by the impact of H^+ at a 75-keV impact energy as a function of the scattering angle. Present theoretical results using different phase factors: solid line, Eq. (21); short-dashed line, Eq. (23); dashed line, Eq. (22); dashed line with +, $V_s(R)\equiv 0$. Experimental data: ●, from Ref. [10].
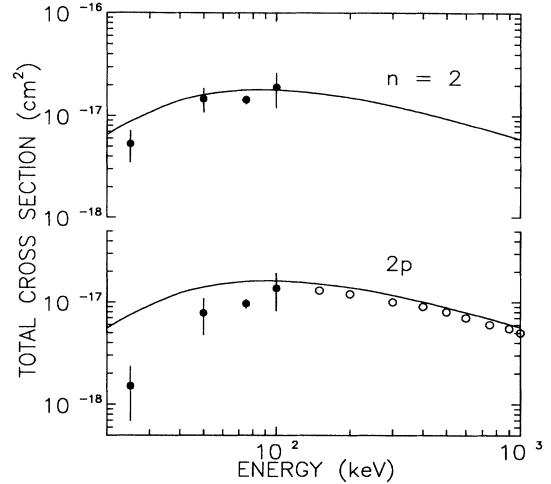

FIG. 4. Total cross section for the single excitation of He to shell $n=2$ and state $nl=2p$ as a function of the projectile energy. Solid line: present results. Experimental data: ●, from Ref. [10]; ○, from Ref. [15].

amplitude is clearly displayed in Fig. 3. There, the differential cross sections for the excitation of the active electron to the state $nl=2s$ at an impact energy of 75 keV are presented for four different exponential factors: the same three as in Figs. 1 and 2 and one further where the static potential is taken as $V_s(\mathbf{R})\equiv 0$ for all internuclear distances R. The noninclusion of the distortions in the projectile trajectory due to interactions of the projectile with the residual target gives a spurious dip in the differential cross sections. A similar behavior is observed for electron capture [12] when inappropriate static potentials are considered. The calculations corresponding to the use of the exponential factors (21) and (23) are again very closed. Even when the SE approximation underestimates the experimental data the best qualitative agreement with experiments is obtained when the most complete exponential factor (21) is used.

In Fig. 4 total cross sections are calculated for excitation of the active electron to the state $nl=2p$ and to the shell $n=2$. As indicated above, distortions in the trajectories due to the interaction between the projectile and the residual target do not influence the total cross sections when the present model is employed. The agreement with experimental data is very good for collision energies of the order or higher than 50 and 100 keV when excitation to $n=2$ and $nl=2p$ is studied, respectively. The theoretical results tend to overestimate the measurements as the impact velocity decreases.

B. Excitation of heavy dielectronic targets

In Figs. 5 and 6 total cross sections are presented as a function of the projectile charge for single-electron excitation of Fe^{24+} and Kr^{34+} colliding with neutral atoms. The neutral atoms play here the role of the projectiles.

One should remark that even if the projectiles are dressed with electrons, we still can apply our present bare-ion model. The screening produced by the extra electrons has been studied in detail by Reinhold and
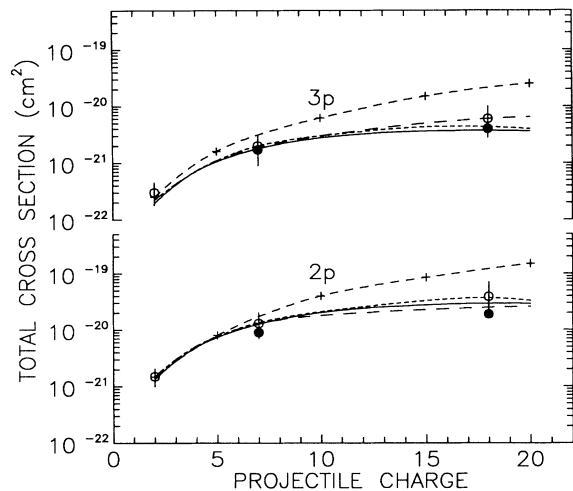
FIG. 5. Total cross section for the single excitation (per electron) of 400-MeV Fe^{24+} to state $nl = 2p$ and $3p$, colliding with neutral atoms of nuclear charge Z_P. Calculations: solid line, present results; dashed line, Schwinger variational [13]; short-dashed line, SE [2]; dashed line with +, B1 [13]. Experimental data: without ($\bullet$) and with ($\circ$) subtraction of transfer ionization, both from Ref. [13].

Miraglia [2]. They estimated an effective projectile charge Z_P^* by using a first-order Born approximation. This effective charge is obtained as a function of the total momentum transfer and takes its minimal value for the zero-scattering angle of the projectile. For excitation of Fe^{24+} ions by the impact of 400-MeV Ar atoms they showed that Z_P^* deviates from Z_P by less than 8%. We have also evaluated the influence of the K-shell electrons of Cu and Zr atoms impacting on Kr^{34+} at a 34-MeV/amu collision energy by using the formulation given by Reinhold and Miraglia and it is easy to prove
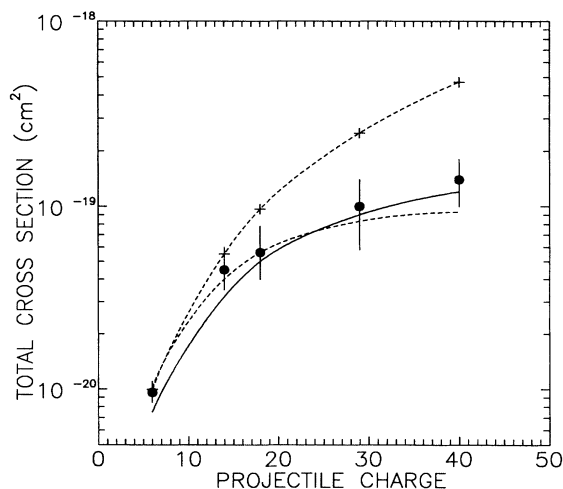

FIG. 6. Total cross section for the single excitation of 34-MeV/amu Kr^{34+} to shell $n = 2$, colliding with neutral atoms of nuclear charge Z_P. Calculations: solid line, present results; dashed line, Schwinger variational [14]; dashed line with +, B1 [14]. Experimental data: $\bullet$, from Ref. [14].

that Z_P is reduced at most to $Z_P^* = 27.23$ and 38.12, respectively.

In Fig. 5 we calculate cross sections for the excitation of the active electron of Fe^{24+} to states $nl = 2p, 3p$ at a total impact energy of 400 MeV. We repeat essentially the calculations of Reinhold and Miraglia [2] but now use an initial orbital energy as indicated in Sec. III. In distinction, the previous authors use a hydrogenic energy $\epsilon_i = -Z_T^{*2}/2$. Comparisons between results obtained with these two different initial orbital energies are in close agreement (see Fig. 5). Further calculations using a first-order Born approximation (B1) and a Schwinger variational model [13] are also included. Experimental data for the impact of He, N, and Ar atoms determined with or without subtraction of double-process mechanisms (simultaneous target ionization and electron capture from the projectile) show a close agreement with our SE calculations.

In Fig. 6 cross sections for the single excitation of the active electron of Kr^{34+} to the state $n = 2$ at a 34-MeV/amu impact energy are presented. Again the SE results are compared with the Schwinger and the B1 calculations [14].

As in the Fe^{24+} case, B1 cross sections overestimate experimental data for the impact of C, Si, Ar, Cu, and Zr atoms, as the projectile charge increases. On the contrary, SE cross sections, which are in close agreement with Schwinger variational calculations, give a good representation of the experiments [14]. Contributions of double-process mechanisms have not been included in the calculations. A rough theoretical estimate of the transfer-ionization reaction has been given in Ref. [14]. It can be also observed from Figs. 5 and 6 that the influence of the projectile electrons will affect the determination of Z_P^* for a region where the total cross section is not so sensitive to the nuclear charge. The agreement between our theoretical model and experiments for these heavy-target reactions is an indication that the presence of the target passive electron does not play a major role for the determination of total cross sections as the target nuclear charge increases.

V. CONCLUSIONS

The symmetric eikonal model previously employed for monoelectronic targets [1] has been extended to the case of the impact of bare ions on dielectronic ions (atoms) at intermediate and high collision velocities. The active electron is assumed to evolve independently of the passive electron even if the last one is considered to influence the initial and final stationary wave function of the excited electron. The passive electron is taken as frozen during the reaction. These approximations are expected to work at high enough impact velocities for which the target relaxation time is longer than the total collision time.

It is shown that the presence of a passive electron affects the trajectory of the projectile and so does the determination of its final angular distribution. Some differences with existing experimental differential cross sections for the impact of protons on a He target at *intermediate collision energies* could be an indication of the

necessity to develop a *two-active*-electron model, where both electrons could evolve during the reaction to a final atomic stationary state. Comparison with total cross sections shows that the model gives a good representation of experiments as the impact velocity increases.

As the charge of the target nucleus becomes larger it can be expected that the passive electron will not play an important role on the excitation reaction. The good agreement between theoretical and experimental total cross sections for the single excitation of Fe^{24+} and Kr^{34+} supports the validity of this expected behavior at intermediate and high collision energies.

*Also at Departamento de Física, Escuela de Ciencias Exactas y Naturales, Facultad de Ciencias Exactas, Ingeniería y Agrimensura, Universidad Nacional de Rosario, Avenida Pellegrini 250, 2000 Rosario, Argentina.

[1] G. R. Deco, P. D. Fainstein, and R. D. Rivarola, J. Phys. B **19**, 213 (1986).

[2] C. O. Reinhold and J. E. Miraglia, J. Phys. B **20**, 1069 (1987).

[3] R. D. Rivarola, R. D. Piacentini, A. Salin, and D. Belkić, J. Phys. B **13**, 2601 (1980).

[4] P. D. Fainstein, V. H. Ponce, and R. D. Rivarola, J. Phys. B **21**, 287 (1988).

[5] J. M. Maidagan and R. D. Rivarola, J. Phys. B **16**, 1211 (1983).

[6] A. Touati, A. Chetioui, M. F. Politis, P. D. Fainstein, R. D. Rivarola, D. Vernhet, and J. P. Rozet (unpublished).

[7] S. E. Corchs, L. J. Dubé, J. M. Maidagan, R. D. Rivarola, and A. Salin, J. Phys. B **25**, 2027 (1992).

[8] P. D. Fainstein, Ph.D. thesis, Instituto Balseiro (Bariloche, Argentina), 1989.

[9] R. McCarroll and A. Salin, J. Phys. B **1**, 163 (1968).

[10] T. J. Kvale, D. G. Seely, D. M. Blankenship, E. Redd, T. J. Gay, M. Kimura, E. Rille, J. L. Peacher, and J. T. Park, Phys. Rev A **32**, 1369 (1985).

[11] C. Clementi and C. Roetti, At. Data Nucl. Data Tables **14**, 445 (1974).

[12] P. J. Martin, K. Arnett, D. M. Blankenship, T. J. Kvale, J. L. Peacher, E. Redd, V. C. Sutcliffe, J. T. Park, C. D. Lin, and J. H. McGuire, Phys. Rev. A **23**, 2858 (1981).

[13] B. Brendlé, R. Gayet, J. P. Rozet, and K. Wohrer, Phys. Rev. Lett. **54**, 2007 (1985).

[14] M. Chabot, P. Nicolai, K. Wohrer, A. Chetioui, J. P. Rozet, M. F. Politis, A. Touati, D. Vernhet, C. Stephan, and R. Gayet, Nucl. Instrum. Methods B **56/57**, 1 (1991).

[15] R. Hippler and K. H. Schartner, J. Phys. B **7**, 618 (1974).